An NMR Confirmation for Increased Folded State Entropy by Loop Truncation

Yulian Gavrilov[1*], Shlomi Dagan[2], Ziv Reich[2], Tali Scherf[3*] and Yaakov Levy[1*]

[1]Department of Structural Biology, [2] Department of Biomolecular Sciences, and [3]Department of Chemical Research Support
Weizmann Institute of Science
Rehovot 76100, Israel

Supporting material

Materials and Methods

1. Sample Preparation

Cloning and purification of the proteins were performed as previously reported [1] using the pET45 system in *Escherichia coli* strain BL2. Uniformly ^{15}N-labeled and ^{15}N,^{13}C-labeled proteins were obtained by growing cells on M9 minimal media supplemented with $^{15}NH_4Cl$ as the sole nitrogen source, and for the doubly-labeled proteins also with ^{13}C-glucose as the sole carbon source. In order to be able to compare our results with the previous resonance assignment of WT hmAcP [2] samples were prepared in 90% H_2O/10% D_2O (V/V), 50 mM phosphate buffer at pH 5.5 with 0.02% of NaN_3.

The final NMR sample concentrations of WT-hmAcP were 170 and 150 μM for the ^{15}N-labeled and ^{15}N,^{13}C-labeled samples, respectively; The Δ6 sample concentrations were 300 and 224 μM for the ^{15}N-labeled and ^{15}N,^{13}C-labeled samples, respectively.

2. NMR Spectroscopy

All NMR experiments were performed on 14.1 T NEO600 and 18.8 T AVANCE III 800 Bruker spectrometers, equipped with 5 mm triple resonance TCI CryoProbes.

2.1. Sequence Assignment

^{1}H-^{15}N HSQC spectra of WT and Δ6 hmAcP were assigned using multi-dimensional triple resonance NMR techniques: initial studies were done at 298 K using ^{15}N-labeled samples (3D ^{15}N-TOCSY and ^{15}N-NOESY spectra). In order to complete the assignment (especially for Δ6) multidimensional triple-resonance HNCA, HNCACB, HN(CO)CA and CBCA(CO)NH spectra were acquired using ^{15}N,^{13}C-labeled samples at 293 K. NMR data for sequential assignment were recorded on a 18.8 T NMR spectrometer.

2.2. Backbone ^{15}N Relaxation Experiments

To probe the backbone dynamics of ^{15}N spins of WT and Δ6 hmAcP, we recorded R_1, $R_{1\rho}$, and {^{1}H}-^{15}N NOE experiments at 293 K on 14.1 and 18.8 T spectrometers (to better restrain the fitting parameters). The R_1 rate constants were determined using nine data points (20–1600 ms, with duplicate data recorded for the first and the last data points to evaluate experimental errors in the peak intensities). The $R_{1\rho}$ rate constants were determined using nine data points (0–144 ms, with duplicate data obtained for the first and last time points). The recycle delay was 3.0 s. Heteronuclear {^{1}H}-^{15}N NOEs were acquired in an interleaved manner using a recycle delay of 10 s (including 7 s of saturation time). The spectral width in the ^{1}H dimension was 16 ppm (9615/12821 Hz for 14.1 T/18.8 T spectrometers, respectively) and in ^{15}N dimension was 31 ppm (2514/1885 Hz), using 4096 and 256 points in the ^{1}H and ^{15}N dimensions, respectively, for R_1 and $R_{1\rho}$; and 4096 and 512 points for {^{1}H}-^{15}N NOE. Measurements of the ^{15}N R_1 and $R_{1\rho}$ rate constants, and heteronuclear {^{1}H}-^{15}N NOEs were performed using standard experimental procedures [3, 4].

2.3. Relaxation Dispersion Experiment

^{15}N CPMG relaxation dispersion experiments [5] for hmAcP Δ6 were recorded at 293 K in a 18.8 T magnetic field using a constant relaxation period T = 40 ms and ν_{CMPG} ranging from 50 to 2000 Hz.

3. Determination of Correlation Times and Order Parameters

NMR data were processed using TopSpin 3.5 (Bruker BioSpin) and CCPN 2.4 release 2 [6]. The analysis of ps–ns dynamics was performed using Dynamics Center 2.4.13 (Bruker BioSpin). Heteronuclear NOE values were calculated as a ratio of peak intensities in the saturated and unsaturated versions of the experiment. T_1 and T_2 values were fitted to monoexponential functions. Errors for T_1, T_2, and NOE were estimated by weighted fit. Calculation of global isotropic correlation time, τ_c, was restricted to residues with NOE > 0.65, residues with T_2 > mean(T2) – 1SD, residues with $[T_2 - \text{mean}(T_2)]/T_2 < [T_1 - \text{mean}(T_1)]/T_1$. For WT, average estimated τ_c is 6.72e-09 s, standard deviation (SD) = 3.27e-10 s. For Δ6, average estimated τ_c is 7.68e-09 s, SD = 5.66e-10 s (based on [7, 8]). Diffusion tensor estimation (D||/D⊥) for WT is 1.18, and for Δ6 is 1.38. Since for Δ6, D||/D⊥ is quite high, we assumed anisotropic tumbling for both WT and Δ6. The method for τ_c and diffusion tensor calculation used in Dynamics Center software is described elsewhere [9].

Relaxation data were analyzed according to the standard [10] and extended [11, 12] Lipari-Szabo model-free (MF) formalism. Average N-H bond length was set to be 1.02 Å and CSA to -160 ppm. Relaxation data were fitted to the five anisotropic motional models using 10000 iteration steps. MF fit parameters: S^2 (MF1); S^2, τ_e (MF2); S^2, R_{ex} (MF3); S^2, τ_e , and R_{ex} (MF4); S^2, S^2_f, and τ_s (MF5). The model implemented in Dynamics Center that best fits a certain residue is regarded as relevant to this residue. However, the final choice of the model for each residue depended of the quality of the fit of the relevant model both for WT and for Δ6. As a criterion of best fit, the Akaike Information Criterion $AIC=\chi^2+2N_{params}$ was used [13, 14]. In addition, we checked how well each MF reproduces T_1 and T_2 independently of NOEs. The optimized MF parameters for all analyzed residues are presented in **Tables S1 and S2**.

We estimated the overall difference between the order parameters for two states of the protein using two measures: weighted mean values of the order parameters and

weighted pairwise RMSD (as it is defined by Solomentsev et al. [15]). The weighted mean values of the order parameters (calculated separately for WT and for Δ6 and then compared) were calculated as:

$$\langle S^2 \rangle = \sum_i \frac{S_i^2}{\sigma_i^2} / \sum_i \left(\frac{1}{\sigma_i^2} \right) \quad (1)$$

where i is a residue index, and σ_i is the standard error of S^2 for residue I [15]. The weighted pairwise RMSD in order parameters between two variants of the protein (WT and Δ6) were calculated as:

$$RMSD = \left(\sum_i \Delta S_i^2 / \sigma_i^2 / \sum_i (1/\sigma_i^2) \right)^{0.5} \quad (2)$$

where i is a residue index, ΔS^2 is the difference in order parameters between the states, and σ_i is the standard error of ΔS^2 for residue i.

Backbone conformational entropy was estimated from the experimental order parameters using the dictionary approach [16].

4. Molecular Dynamics Simulations

The variants of AcP protein were studied using all-atom molecular dynamics simulations withGROMACS version 4.5.4 [17] and AMBER99SB-ILDN force field [18]. For each system (*i.e.,* the unmodified WT and the truncated version, Δ6), we preformed 4–5 simulations for 500 ns. Thus, each protein system was studied for 2–2.5 μs (see [19] for further details). The iRED method was used to extract backbone N-H order parameters [20]. The calculations were performed for 6 ns trajectory blocks. The final order parameter values represent the averages over these blocks. Conformational entropy was estimated based on distributions of the backbone dihedral angles (ϕ, ψ) and/or side chain χ angles (for side chain entropy):

$$S = -kT \sum_j \sum_i^N p_j(ai) ln p_j(ai) \quad (3)$$

where the sum is over the N bins of the dihedral angle αi of residue j, and p is the population of the i^{th} bin. The angles were discretized in different bin sizes; convergence was reached with a bin size of 6°. The ΔS was calculated by the difference $S^{\Delta 6}$-S^{WT}. This

or similar methods for estimating protein conformational entropy were successfully applied in different studies [15, 21, 22, 23, 24, 25, 26, 27, 28].

Table S1. Model-free parameters for hmAcP WT.

Residue	MF type	S^2(all M)	error	S^2_f(M5)	error	τ_e/S(M4/5)	error	R_{ex}(M3/4)	error	dR_1[%]	dR_2[%]	dNOE[%]
1M	M5	0.2430	0.0162	0.8320	0.0155	2.93E-10	1.51E-11			8.97	2.09	-46.40
2S	NaN	NaN	NaN									
3T	M2	0.6230	0.0068			6.55E-11	3.45E-12			15.70	23.80	15.10
4A	M2	0.9900	0.0024			8.23E-10	2.60E-08			556.00	899.00	-119.00
5Q	M2	0.2960	0.0033			4.19E-10	2.65E-12			8.78	4.13	-502.00
6S	M5	0.4280	0.0051	0.9760	0.0050	5.91E-10	8.67E-12			6.79	4.34	36.60
7L	M5	0.8160	0.0136	0.9360	0.0104	2.85E-10	6.81E-11			19.30	9.28	0.56
8K	M5	0.8070	0.0152	0.9660	0.0149	7.92E-10	1.20E-10			13.90	6.28	3.77
9S	M2	0.8480	0.0119			3.95E-10	3.45E-11			17.50	1.31	20.30
10V	M5	0.9900	0.0248	0.9900	0.0139	2.52E-09	2.88E-04			17.50	2.91	14.80
11D	M5	0.8490	0.0184	0.9690	0.0157	8.31E-10	1.72E-10			17.60	8.29	3.34
12Y	M5	0.9440	0.0153	0.9980	0.0109	3.72E-10	1.76E-10			17.10	7.13	1.56
13E	M5	0.8820	0.0143	0.9590	0.0095	3.35E-10	1.02E-10			15.50	5.26	1.62
14V	M5	0.8110	0.0224	0.9670	0.0172	6.74E-10	1.21E-10			14.90	7.41	5.77
15F	M4	0.9050	0.0122			5.87E-11	2.10E-11	0.1030	0.2770	18.90	6.30	3.56
16G	M5	0.8280	0.0166	0.9410	0.0125	5.82E-10	1.07E-10			14.30	5.69	3.74
17R	M5	0.8550	0.0098			3.25E-11	1.04E-11	0.3470	0.2470	16.80	7.27	2.17
18V	M5	0.7370	0.0164	0.8770	0.0169	9.23E-10	1.88E-10			14.90	8.59	3.58
19Q	NaN	NaN	NaN									
20G	M4	0.8540	0.0127			4.36E-11	1.45E-11	1.3400	0.3760	17.20	6.04	1.39
21V	M4	0.8620	0.0253			1.20E-10	4.98E-11	1.2800	0.6220	17.40	8.50	19.10
22S	M4	0.9360	0.0365			1.52E-10	2.06E-10	5.6300	1.1700	16.30	16.90	5.49
23F	M5	0.8840	0.0795	0.9490	0.0382	2.75E-09	6.30E-09			17.60	15.10	10.60
24R	M5	0.8320	0.0136			4.02E-11	1.05E-11	1.4700	0.3960	13.60	4.83	0.55
25M	NaN	NaN	NaN									
26Y	M4	0.8780	0.0074			2.38E-11	9.14E-12	1.5000	0.2080	18.00	3.77	0.69
27T	M4	0.8660	0.0063			6.57E-11	8.00E-12	1.8600	0.1910	19.10	4.89	2.11
28E	M4	0.8790	0.0069			7.07E-11	1.02E-11	2.0100	0.1780	18.10	5.17	0.84
29D	M2	0.9900	0.0225			4.62E-10	2.02E-07			8.61	8.94	18.10

30E	M4	0.8710	0.0052			7.91E-11	7.63E-12	1.4600	0.1340	17.30	5.02	1.78
31A	M4	0.8800	0.0053			4.47E-11	6.91E-12	1.6500	0.1490	17.60	0.82	0.09
32R	M4	0.8460	0.0054			4.45E-11	5.50E-12	2.1900	0.1590	19.10	12.00	2.72
33K	M4	0.8300	0.0048			2.49E-11	4.62E-12	2.2400	0.1270	18.60	3.88	3.98
34I	M4	0.8540	0.0069			4.36E-11	7.23E-12	0.8750	0.2460	18.90	15.90	1.91
35G	M2	0.8750	0.0075			2.77E-11	1.02E-11			19.20	16.40	2.02
36V	M4	0.8460	0.0066			3.44E-11	7.19E-12	0.7030	0.1470	19.70	5.85	23.00
37V	M5	0.8240	0.0177	0.9620	0.0169	9.55E-10	1.94E-10			15.20	5.99	3.88
38G	M5	0.8480	0.0227	0.9740	0.0215	1.06E-09	3.18E-10			14.20	6.43	3.03
39W	M4	0.8050	0.0170			1.10E-09	7.19E-11	0.6310	0.2200	12.30	5.82	0.21
40V	M5	0.8620	0.0193	0.9990	0.0206	1.02E-09	2.71E-10			13.80	5.63	2.54
41K	M5	0.8450	0.0193	0.9840	0.0156	7.30E-10	1.33E-10			14.20	5.73	5.86
42N	M5	0.8640	0.0367	0.9050	0.0295	1.94E-09	4.14E-09			18.10	7.68	7.84
43T	M4	0.8770	0.0099			1.16E-10	2.03E-11	0.0308	0.2450	17.10	6.76	0.08
44S	NaN	NaN	NaN									
45K	M4	0.7960	0.0062			5.11E-11	5.18E-12	0.8600	0.1550	18.30	5.07	1.18
46G	M5	0.7350	0.0136	0.9120	0.0116	7.76E-10	7.76E-11			13.70	6.93	6.26
47T	M5	0.8230	0.0185	0.9430	0.0158	8.31E-10	1.73E-10			15.40	7.02	3.29
48V	M4	0.8320	0.0250			4.94E-10	4.37E-11	0.3380	0.3160	17.90	5.93	14.10
49T	M2	0.9290	0.0089			1.16E-10	3.34E-11			19.20	3.57	3.47
50G	M5	0.9510	0.0209	0.9510	0.0132	2.16E-09	2.50E-06			19.80	0.91	13.30
51Q	M2	0.9380	0.0120			5.88E-10	8.19E-11			13.50	12.60	7.35
52V	M5	0.8170	0.0153	0.9520	0.0142	7.79E-10	1.36E-10			14.80	6.64	3.93
53Q	M5	0.8310	0.0159	0.9460	0.0147	7.80E-10	1.61E-10			14.40	4.75	4.05
54G	M5	0.8150	0.0142	0.9790	0.0106	6.49E-10	7.08E-11			14.30	5.64	6.94
55P	NaN	NaN	NaN									
56E	M2	0.9900	0.0149			6.41E-10	4.64E-07			16.30	4.10	8.43
57D	M4	0.8560	0.0053			6.65E-11	6.66E-12	1.8200	0.1320	19.00	0.63	1.58
58K	M4	0.8770	0.0065			3.44E-11	7.97E-12	0.9990	0.1680	18.10	5.11	2.39
59V	M4	0.8570	0.0060			1.50E-11	6.77E-12	1.8000	0.1590	17.90	5.33	0.46
60N	M4	0.8330	0.0050			1.84E-11	5.01E-12	2.7000	0.1390	17.90	3.14	0.23
61S	M4	0.8390	0.0044			3.76E-11	4.57E-12	1.9000	0.1190	17.90	1.41	0.39

62M	M4	0.8680	0.0061			7.57E-11	8.45E-12	1.4000	0.1630	17.90	4.32	0.94
63K	M4	0.8320	0.0074			5.14E-11	7.51E-12	2.3500	0.1690	20.00	4.81	4.62
64S	M4	0.8800	0.0050			2.83E-11	6.38E-12	0.9890	0.1240	18.30	5.39	0.73
65W	M4	0.8850	0.0068			6.40E-11	9.96E-12	1.8000	0.1670	18.40	4.89	1.28
66L	M4	0.8270	0.0073			5.35E-11	7.00E-12	2.0900	0.2140	18.20	0.26	0.16
67S	M4	0.8450	0.0061			2.66E-11	6.36E-12	0.7700	0.1810	18.70	10.20	1.63
68K	M4	0.8710	0.0091			6.23E-11	1.14E-11	0.4990	0.2020	20.40	5.51	3.14
69V	M5	0.8680	0.0161	0.9550	0.0135	2.51E-10	1.11E-10			16.00	4.49	2.80
70G	NaN	NaN	NaN									
71S	M4	0.9270	0.0094			1.25E-10	3.90E-11			16.80	4.44	0.13
72P	NaN	NaN	NaN									
73S	M5	0.8380	0.0140	0.9080	0.0094	5.43E-10	1.33E-10			17.50	9.89	2.10
74S	M4	0.8420	0.0045			1.96E-11	4.60E-12	2.1600	0.1120	17.90	3.70	0.21
75R	M5	0.8140	0.0206	0.9190	0.0202	1.38E-09	5.46E-10			15.10	9.88	3.08
76I	M5	0.7750	0.0170	0.8890	0.0115	5.47E-10	1.00E-10			16.00	8.83	3.26
77D	M5	0.7910	0.0296	0.9320	0.0277	1.23E-09	4.48E-10			13.70	6.83	2.97
78R	M5	0.7740	0.0085	0.9370	0.0079	6.54E-10	5.26E-11			15.50	8.18	5.81
79T	M5	0.7790	0.0113	0.9020	0.0086	4.81E-10	6.08E-11			14.80	5.27	6.05
80N	M5	0.7850	0.0175	0.9210	0.0160	8.53E-10	1.69E-10			14.70	7.56	3.13
81F	M5	0.7640	0.0159	0.9360	0.0154	8.54E-10	1.23E-10			12.50	5.49	3.73
82S	M5	0.8010	0.0156	0.9370	0.0146	7.94E-10	1.35E-10			14.30	6.99	3.96
83N	M5	0.7750	0.0141	0.8970	0.0146	1.09E-09	2.37E-10			14.00	6.30	2.83
84E	M5	0.8190	0.0078	0.9720	0.0067	6.08E-10	4.44E-11			16.50	8.17	4.12
85K	M5	0.8780	0.0211	0.9430	0.0221	1.06E-09	6.61E-10			16.30	6.52	3.72
86T	M5	0.7890	0.0098	0.8670	0.0085	5.43E-10	1.07E-10			18.10	10.80	0.14
87I	M5	0.8310	0.0153	0.9500	0.0128	6.21E-10	1.19E-10			16.80	11.40	1.46
88S	M5	0.8070	0.0152	0.9040	0.0170	1.25E-09	4.41E-10			14.90	6.27	2.51
89K	M5	0.8120	0.0094	0.9080	0.0093	7.78E-10	1.25E-10			18.10	7.76	1.81
90L	M4	0.8270	0.0065			4.19E-11	6.02E-12	0.6950	0.1560	17.30	5.83	1.34
91E	M5	0.7930	0.0178	0.9270	0.0138	6.36E-10	1.06E-10			15.50	7.56	3.87
92Y	M5	0.7930	0.0106	0.8820	0.0079	4.28E-10	7.82E-11			18.00	9.03	1.79
93S	M4	0.8560	0.0119			2.98E-11	1.20E-11	0.1280	0.3070	18.50	7.09	2.53

94N	M5	0.7590	0.0103	0.9360	0.0097	7.43E-10	6.65E-11			14.80	7.18	4.19
95F	M5	0.7480	0.0150	0.8540	0.0156	1.01E-09	2.62E-10			14.60	6.59	3.18
96S	M5	0.8050	0.0147	0.9230	0.0179	1.23E-09	3.73E-10			14.10	6.02	4.91
97I	M5	0.7470	0.0127	0.9120	0.0102	5.86E-10	6.09E-11			14.60	6.88	4.78
98R	M5	0.8550	0.0207	0.9530	0.0159	5.57E-10	1.57E-10			16.30	7.34	2.05
99Y	M2	0.7460	0.0050			2.27E-11	3.34E-12			18.30	17.90	6.36

Tables S2. Model-free parameters for hmAcP Δ6.

Residue	MF type	S^2(all M)	error	S^2_f (M5)	error	τ_e/S(M4/5)	error	R_{ex}(M3/4)	error	dR_1[%]	dR_2[%]	dNOE[%]
1M	M5	0.0879	0.0102	0.6900	0.0145	2.47E-10	1.04E-11			3.95	13.90	-32.30
2S	M5	0.0861	0.0019	0.8800	0.0032	3.61E-10	2.06E-12			6.32	1.03	-55.90
3T	M2	0.1520	0.0021			4.54E-10	1.73E-12			10.30	15.00	-109.00
4A	M2	0.2410	0.0020			4.82E-10	1.68E-12			5.67	4.79	-252.00
5Q	M2	0.3290	0.0023			4.82E-10	2.26E-12			7.35	3.39	190.00
6S	M5	0.4180	0.0036	0.9730	0.0045	6.89E-10	8.16E-12			4.86	4.94	28.40
7L	M5	0.8520	0.0093	0.9530	0.0068	3.28E-10	4.92E-11			17.20	4.30	2.36
8K	M5	0.8920	0.0084	0.9390	0.0234	1.47E-10	1.56E-10			17.30	6.21	0.19
9S	M2	0.8620	0.0046			1.75E-11	6.28E-12			18.30	13.50	4.51
10V	M5	0.8210	0.0113	0.9990	0.0108	9.63E-10	9.05E-11			12.40	5.90	3.68
11D	M5	0.8300	0.0139	0.9690	0.0127	9.50E-10	1.30E-10			12.50	4.97	3.20
12Y	M5	0.9300	0.0094	0.9740	0.0072	4.22E-10	1.44E-10			18.10	8.21	1.01
13E	M5	0.7580	0.0101	0.9080	0.0110	1.21E-09	1.64E-10			9.56	6.28	2.48
14V	M5	0.8680	0.0165	0.9620	0.0140	8.21E-10	1.82E-10			12.80	3.06	2.65
15F	M4	0.9330	0.0124			1.03E-10	3.42E-11	2.9800	0.3020	20.60	5.27	0.05
16G	NaN	NaN	NaN									
17R	NaN	NaN	NaN									
18V	NaN	NaN	NaN									
19Q	M4	0.8460	0.0127			9.22E-11	1.90E-11	7.1900	0.2980	17.10	12.90	11.80
20G	NaN	NaN	NaN									
21V	NaN	NaN	NaN									
22S	M4	0.8750	0.0154			1.24E-10	3.39E-11	5.6500	0.3530	17.60	10.50	1.93
23F	NaN	NaN	NaN									
24R	NaN	NaN	NaN									
25M	M4	0.9140	0.0096			6.76E-11	1.41E-11	0.6470	0.1750	20.30	9.00	0.81
26Y	M4	0.8440	0.0069			2.74E-11	5.18E-12	3.7000	0.1720	17.70	4.54	1.00
27T	M4	0.8420	0.0078			2.34E-11	6.32E-12	3.2800	0.1720	18.70	6.72	0.63
28E	M4	0.8170	0.0084			2.19E-11	5.71E-12	3.4700	0.2020	19.00	5.79	0.01
29D	M5	0.9600	0.0059			1.30E-10	3.96E-11			0.00	0.02	0.03

30E	M4	0.9310	0.0065			2.91E-11	1.14E-11	1.0800	0.1470	18.50	5.71	0.48
31A	M4	0.9070	0.0060			4.70E-11	7.64E-12	1.4000	0.1370	18.40	5.77	1.14
32R	M4	0.8130	0.0055			2.85E-11	3.64E-12	3.2900	0.1370	14.90	3.39	2.97
33K	M4	0.8020	0.0040			2.11E-11	2.86E-12	2.8800	0.0980	17.00	2.70	0.94
34I	M4	0.8930	0.0059			5.48E-11	7.32E-12	0.9060	0.1370	19.60	5.14	2.29
35G	M2	0.9260	0.0074			4.10E-11	1.24E-11			18.70	4.49	0.75
36V	M4	0.8520	0.0054			3.82E-11	4.88E-12	0.3820	0.1290	19.00	5.95	1.19
37V	M5	0.7800	0.0120	0.9430	0.0118	9.45E-10	1.05E-10			11.60	5.52	3.79
38G	M5	0.7870	0.0159	0.9790	0.0141	9.52E-10	1.03E-10			10.30	3.98	4.08
39W	M4	0.9220	0.0126			6.07E-10	5.36E-11	0.3590	0.1650	15.40	6.35	1.53
40V	M5	0.6990	0.0236	0.9260	0.0059	3.86E-09	1.08E-09			13.50	7.10	3.68
41K	M5	0.8820	0.0163	0.9680	0.0114	5.52E-10	1.14E-10			15.10	5.31	2.18
42N	M5	0.8490	0.0174	0.9580	0.0130	6.02E-10	1.03E-10			12.90	4.76	3.01
43T	M4	0.8510	0.0183			5.65E-10	4.43E-11	3.2800	0.2770	15.50	6.81	3.05
44S	NaN	NaN	NaN									
45K	M4	0.8570	0.0167			1.30E-10	3.22E-11	2.0100	0.2840	18.50	15.50	3.01
46G	NaN	NaN	NaN									
47T	NaN	NaN	NaN									
48V	M4	0.9010	0.0443			6.14E-10	1.87E-10	5.3400	0.6370	15.30	10.10	0.93
49T	M2	0.9560	0.0066			2.64E-09	1.52E-09			14.80	25.00	16.10
50G	M5	0.8590	0.0099	0.9390	0.0079	8.23E-10	1.17E-10			14.80	5.69	2.49
51Q	M2	0.9140	0.0066			5.83E-10	4.63E-11			14.30	7.60	0.80
52V	M5	0.7990	0.0097	0.9450	0.0109	9.18E-10	1.13E-10			11.30	6.31	3.22
53Q	M5	0.8310	0.0092	0.9480	0.0081	5.08E-10	5.83E-11			13.40	6.21	4.11
54G	M5	0.8410	0.0120	0.9710	0.0104	9.87E-10	1.19E-10			12.70	2.48	2.61
55P	NaN	NaN	NaN									
56E	M2	0.9150	0.0052			5.41E-11	9.29E-12			0.06	0.23	0.27
57D	M4	0.9070	0.0041			2.94E-11	5.68E-12	0.6030	0.0955	17.80	4.23	0.69
58K	M4	0.8530	0.0051			2.75E-11	4.48E-12	1.0100	0.1230	18.00	4.15	2.03
59V	M4	0.8370	0.0043			3.21E-11	3.86E-12	2.5300	0.1320	18.00	4.09	0.13
60N	M4	0.9230	0.0052			3.16E-11	7.35E-12	0.4090	0.1220	17.80	8.56	0.15
61S	M4	0.8080	0.0041			2.33E-11	2.89E-12	2.8800	0.0911	17.90	4.08	0.57

62M	M4	0.9000	0.0055			3.54E-11	6.73E-12	1.8700	0.1420	17.90	3.54	0.48
63K	M4	0.8330	0.0052			3.26E-11	4.27E-12	2.7200	0.1310	17.30	4.93	1.53
64S	M4	0.8450	0.0047			2.51E-11	3.78E-12	1.7000	0.0940	17.80	5.82	0.57
65W	M4	0.9270	0.0061			2.78E-11	9.69E-12	0.7830	0.1340	18.20	5.51	0.74
66L	M4	0.8580	0.0070			8.47E-12	6.10E-12	1.5900	0.1360	15.80	6.56	1.82
67S	M4	0.8830	0.0054			4.02E-11	5.18E-12	1.8700	0.1340	20.70	4.69	2.01
68K	M4	0.9110	0.0061			8.86E-11	1.15E-11	0.5990	0.1300	19.00	5.71	1.02
69V	M5	0.8810	0.0091	0.9750	0.0093	2.46E-10	6.17E-11			19.30	8.73	0.62
70G	M5	0.8600	0.0090	0.9600	0.0065	3.27E-10	4.56E-11			18.00	4.51	2.91
71S	NaN	NaN	NaN									
72P	NaN	NaN	NaN									
73S	NaN	NaN	NaN									
74S	NaN	NaN	NaN									
75R	NaN	NaN	NaN									
76I	NaN	NaN	NaN									
77D	M5	0.7510	0.0098	0.9490	0.0113	8.75E-10	8.31E-11			11.80	5.24	4.63
78R	M5	0.8870	0.0067	0.9820	0.0587	9.80E-11	9.28E-11			19.80	8.19	4.12
79T	M5	0.7740	0.0083	0.9190	0.0069	5.47E-10	3.97E-11			14.90	5.30	4.20
80N	M5	0.8570	0.0172	0.9510	0.0142	6.78E-10	1.59E-10			17.90	8.46	2.03
81F	M5	0.7200	0.0107	0.8840	0.0100	8.10E-10	7.23E-11			13.20	7.61	5.17
82S	NaN	NaN	NaN									
83N	M5	0.6820	0.0088	0.8830	0.0103	1.24E-09	1.23E-10			7.35	6.79	3.65
84E	M5	0.7370	0.0052	0.9510	0.0058	9.51E-10	4.06E-11			7.94	4.92	4.51
85K	M5	0.8290	0.0134	0.9790	0.0121	7.87E-10	9.50E-11			13.40	7.70	3.50
86T	M5	0.7270	0.0060	0.8980	0.0062	7.10E-10	3.86E-11			13.40	7.20	4.96
87I	M5	0.7710	0.0101	0.9320	0.0129	1.22E-09	1.96E-10			11.30	6.24	2.40
88S	M5	0.8300	0.0070	0.9050	0.0072	5.65E-10	9.10E-11			17.50	7.67	2.19
89K	M5	0.7440	0.0051	0.9120	0.0063	8.95E-10	5.41E-11			11.80	6.74	4.03
90L	M4	0.8210	0.0058			4.19E-11	4.07E-12	1.3100	0.1370	17.30	3.76	2.00
91E	M5	0.7860	0.0102	0.9350	0.0108	8.10E-10	9.57E-11			12.10	3.98	5.11
92Y	M5	0.7690	0.0069	0.8950	0.0060	5.23E-10	4.02E-11			15.70	6.49	3.59
93S	M4	0.7960	0.0091			2.60E-11	4.99E-12	1.0600	0.2250	16.40	6.15	2.38

94N	M5	0.7150	0.0057	0.9090	0.0072	1.08E-09	7.13E-11			10.20	6.95	4.04
95F	M5	0.7030	0.0100	0.8880	0.0120	1.40E-09	2.03E-10			8.20	6.38	2.34
96S	M5	0.7350	0.0097	0.9140	0.0116	1.31E-09	1.76E-10			9.94	5.96	3.21
97I	M5	0.6930	0.0086	0.8780	0.0091	8.92E-10	6.80E-11			11.50	5.38	4.82
98R	M5	0.6840	0.0122	0.8990	0.0134	1.29E-09	1.56E-10			7.47	5.74	3.38
99Y	M2	0.8170	0.0046			5.69E-11	3.82E-12			17.40	1.11	0.44

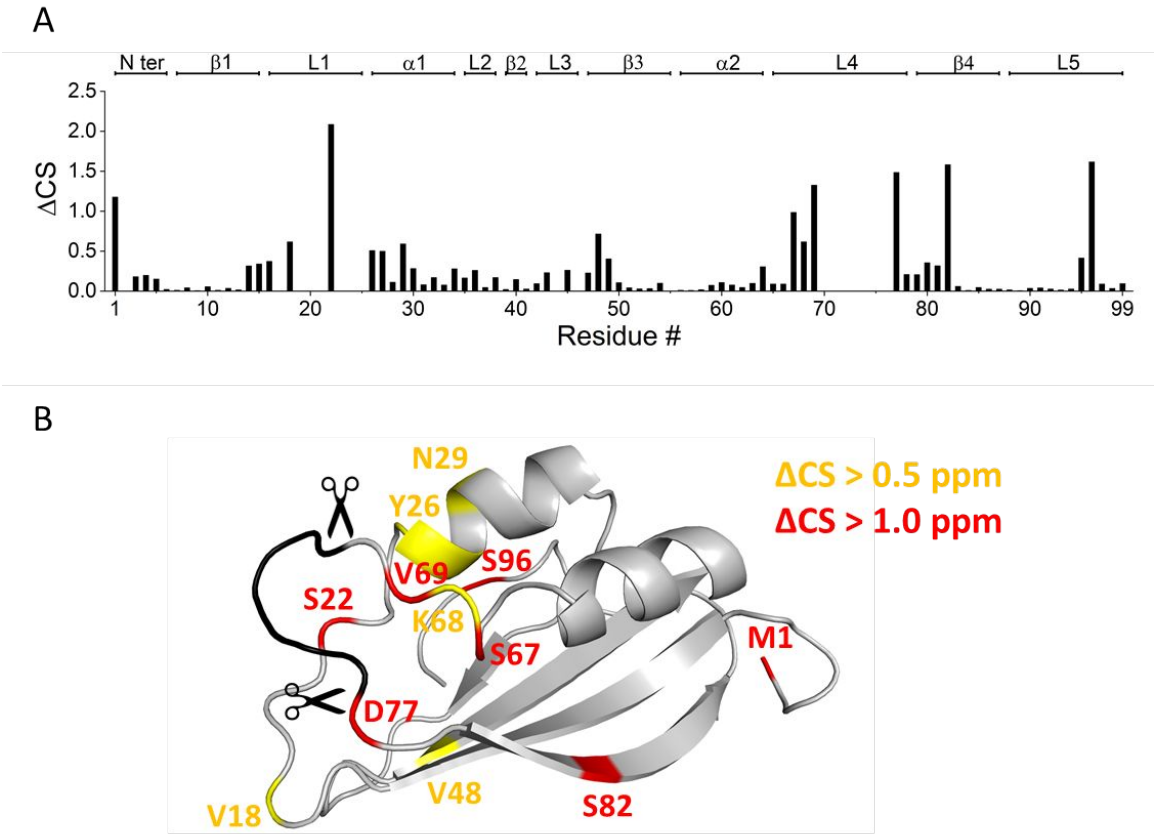

Figure S1. (**A**) Chemical shift difference (ΔCS) between peaks in the H-N HSQC spectra of the wild type (WT) and truncated Δ6 variant of hmAcP. $\Delta CS=((\Delta\delta H)^2+(0.14\ \Delta\delta N)^2)^{0.5}$, where ΔδH and ΔδN are the ^1H and ^{15}N chemical shift differences: ΔδH= δH(Δ6)-δH(WT) and ΔδN= δN(Δ6)-δN(WT), respectively. **(B)** Residues with the highest chemical shift difference are shown on the structure of WT hmAcP. Residues are shown in yellow if 0.5 ppm < ΔCS < 1 ppm and in red if ΔCS > 1 ppm. Truncated residues in L4 (Δ6) are shown in black; the boarders of the truncated region are indicated by the scissors sign. The homology model of hmAcP is based on the solution structure of the horse orthologue of hmAcP (PDB code: 1APS, [29]).

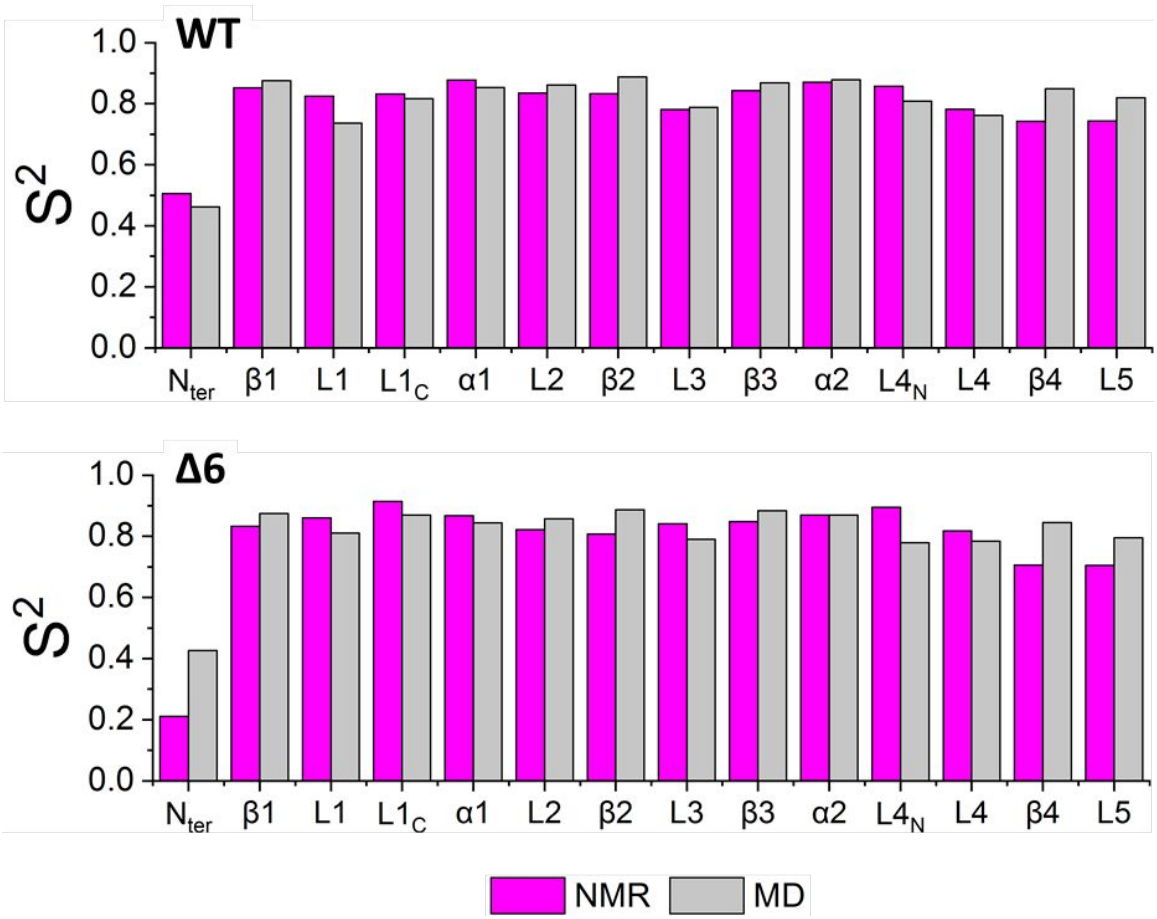

Figure S2. Squared generalized order parameters for backbone N-H groups (S^2) derived from NMR (magenta) and molecular dynamics (MD; gray) data for wile type (WT; upper panel) and truncated Δ6 (lower panel) variants of the hmAcP protein. Data are presented as the sum per structural element from the N-terminal (Nter). $L1_C$ and $L4_N$ are helical-like parts of L1 and L4, respectively.

References

1. Dagan, S.; Hagai, T.; Gavrilov, Y.; Kapon, R.; Levy, Y.; Reich, Z., Stabilization of a protein conferred by an increase in folded state entropy. *P Natl Acad Sci USA* **2013,** *110* (26), 10628-33.
2. Fusco, G.; De Simone, A.; Hsu, S. T.; Bemporad, F.; Vendruscolo, M.; Chiti, F.; Dobson, C. M., (1)H, (1)(3)C and (1)(5)N resonance assignments of human muscle acylphosphatase. *Biomolecular NMR assignments* **2012,** *6* (1), 27-9.
3. Farrow, N. A.; Muhandiram, R.; Singer, A. U.; Pascal, S. M.; Kay, C. M.; Gish, G.; Shoelson, S. E.; Pawson, T.; Formankay, J. D.; Kay, L. E., Backbone dynamics of a free and a phosphopeptide-complexed Src homology-2 domain studied by N-15 NMR relaxation. *Biochemistry-Us* **1994,** *33* (19), 5984-6003.
4. Skelton, N. J.; Palmer, A. G.; Akke, M.; Korde, l. J.; Rance, M.; Chazin, W. J., Practical aspects of two-dimensional proton-detected 15n spin relaxation measurements. *JMR B* **1993,** *102* (3), 253-264.
5. Hansen, D. F.; Vallurupalli, P.; Kay, L. E., An improved 15N relaxation dispersion experiment for the measurement of millisecond time-scale dynamics in proteins. *The journal of physical chemistry. B* **2008,** *112* (19), 5898-904.
6. Vranken, W. F.; Boucher, W.; Stevens, T. J.; Fogh, R. H.; Pajon, A.; Llinas, P.; Ulrich, E. L.; Markley, J. L.; Ionides, J.; Laue, E. D., The CCPN data model for NMR spectroscopy: Development of a software pipeline. *Proteins* **2005,** *59* (4), 687-696.
7. Kay, L. E.; Torchia, D. A.; Bax, A., Backbone dynamics of proteins as studied by N-15 inverse detected heteronuclear nmr-spectroscopy - application to staphylococcal nuclease. *Biochemistry-Us* **1989,** *28* (23), 8972-8979.
8. Fushman, D.; Weisemann, R.; Thuring, H.; Ruterjans, H., Backbone dynamics of ribonuclease-t1 and its complex with 2'gmp studied by 2-dimensional heteronuclear NMR-spectroscopy. *J Biomol Nmr* **1994,** *4* (1), 61-78.
9. Fushman, D., *BioNMR in drug research*. Wiley-VCH: Weinheim, 2002.
10. Lipari, G.; Szabo, A., Model-free approach to the interpretation of nuclear magnetic-resonance relaxation in macromolecules .2. analysis of experimental results. *J Am Chem Soc* **1982,** *104* (17), 4559-4570.
11. Clore, G. M.; Szabo, A.; Bax, A.; Kay, L. E.; Driscoll, P. C.; Gronenborn, A. M., Deviations from the simple 2-parameter model-free approach to the interpretation of n-15 nuclear magnetic-relaxation of proteins. *J Am Chem Soc* **1990,** *112* (12), 4989-4991.
12. Clore, G. M.; Driscoll, P. C.; Wingfield, P. T.; Gronenborn, A. M., Analysis of the backbone dynamics of interleukin-1-beta using 2-dimensional inverse detected heteronuclear N-15-H-1 NMR-spectroscopy. *Biochemistry-Us* **1990,** *29* (32), 7387-7401.
13. Chen, J. H.; Brooks, C. L.; Wright, P. E., Model-free analysis of protein dynamics: assessment of accuracy and model selection protocols based on molecular dynamics simulation. *J Biomol Nmr* **2004,** *29* (3), 243-257.

14. Akaike, H., Citation classic - a new look at the statistical-model identification. *Cc/Eng Tech Appl Sci* **1981,** (51), 22-22.
15. Solomentsev, G.; Diehl, C.; Akke, M., Conformational entropy of fk506 binding to fkbp12 determined by nuclear magnetic resonance relaxation and molecular dynamics simulations. *Biochemistry-Us* **2018,** *57* (9), 1451-1461.
16. Li, D. W.; Bruschweiler, R., A dictionary for protein side-chain entropies from NMR order parameters. *J Am Chem Soc* **2009,** *131* (21), 7226-7.
17. Hess, B.; Kutzner, C.; van der Spoel, D.; Lindahl, E., GROMACS 4: Algorithms for highly efficient, load-balanced, and scalable molecular simulation. *J Chem Theory Comput* **2008,** *4* (3), 435-447.
18. Lindorff-Larsen, K.; Piana, S.; Palmo, K.; Maragakis, P.; Klepeis, J. L.; Dror, R. O.; Shaw, D. E., Improved side-chain torsion potentials for the Amber ff99SB protein force field. *Proteins* **2010,** *78* (8), 1950-8.
19. Gavrilov, Y.; Dagan, S.; Levy, Y., Shortening a loop can increase protein native state entropy. *Proteins* **2015,** *83* (12), 2137-2146.
20. Prompers, J. J.; Bruschweiler, R., General framework for studying the dynamics of folded and nonfolded proteins by NMR relaxation spectroscopy and MD simulation. *J Am Chem Soc* **2002,** *124* (16), 4522-34.
21. Baxa, M. C.; Haddadian, E. J.; Jumper, J. M.; Freed, K. F.; Sosnick, T. R., Loss of conformational entropy in protein folding calculated using realistic ensembles and its implications for NMR-based calculations. *P Natl Acad Sci USA* **2014,** *111* (43), 15396-15401.
22. Baxa, M. C.; Haddadian, E. J.; Jha, A. K.; Freed, K. F.; Sosnick, T. R., Context and force field dependence of the loss of protein backbone entropy upon folding using realistic denatured and native state ensembles. *J Am Chem Soc* **2012,** *134* (38), 15929-15936.
23. Numata, J.; Knapp, E. W., Balanced and bias-corrected computation of conformational entropy differences for molecular trajectories. *J Chem Theory Comput* **2012,** *8* (4), 1235-1245.
24. Solomentsev, G. Y.; English, N. J.; Mooney, D. A., Effects of external electromagnetic fields on the conformational sampling of a short alanine peptide. *J Comput Chem* **2012,** *33* (9), 917-923.
25. Harpole, K. W.; Sharp, K. A., Calculation of configurational entropy with a boltzmann-quasiharmonic model: the origin of high-affinity protein-ligand binding. *Journal of Physical Chemistry B* **2011,** *115* (30), 9461-9472.
26. Diehl, C.; Genheden, S.; Modig, K.; Ryde, U.; Akke, M., Conformational entropy changes upon lactose binding to the carbohydrate recognition domain of galectin-3. *J Biomol Nmr* **2009,** *45* (1-2), 157-169.
27. Li, D. W.; Showalter, S. A.; Bruschweiler, R., Entropy localization in proteins. *The journal of physical chemistry. B* **2010,** *114* (48), 16036-44.
28. Li, D. W.; Bruschweiler, R., In silico relationship between configurational entropy and soft degrees of freedom in proteins and peptides. *Physical review letters* **2009,** *102* (11), 118108.
29. Pastore, A.; Saudek, V.; Ramponi, G.; Williams, R. J., Three-dimensional structure of acylphosphatase. Refinement and structure analysis. *J Mol Biol* **1992,** *224* (2), 427-40.